PHYSICAL REVIEW B VOLUME 18, NUMBER 12 15 DECEMBER 1978

Modes for transmission of microwaves through alkali metals at cryogenic temperatures

Daniel Pinkel,* Gerald L. Dunifer,† and Sheldon Schultz
University of California at San Diego, La Jolla, California 92093
(Received 4 April 1977)

We present experimental results for three different modes of magnetic-field-dependent microwave transmission through thin foils of pure alkali metals at cryogenic temperatures. The first of these modes occurs when the magnetic field is parallel to the surface, and results in propagation windows above the field for cyclotron resonance H_c and its subharmonics. The mode is identified as the transmission analog of cyclotron waves as observed in reflection. The data are compared with extensive computer simulations in an effort to deduce values for the coefficients of the momentum part of the Landau correlation function. Results are presented for Na, K, and Rb, and compared with other values. The second mode contains two series, each characterized by a rapid oscillatory dependence of the transmitted field on the angle between the applied dc magnetic field and the sample surface. They occur when the dc field is much greater than H_c. We identify one of these series with a model dependent upon the simple time of flight for electrons along the field lines. The other appears to be more complicated and we suggest warrants theoretical attention. The third mode, for the dc field normal to the sample, is identified as the Gantmakher-Kaner oscillations at microwave frequencies. Attention is focused on the behavior of this mode near H_c and for fields much greater than H_c. The signal-to-noise ratio available experimentally for observation of all of the modes discussed is very high. Consequently it is suggested that if any electronic properties of interest of the alkali metals can be theoretically identified with an observed mode, they could be further measured and analyzed.

I. INTRODUCTION

As is well known, the propagation of microwaves (≈10 GHz) through thin foils of normal metals at room temperature is exponentially attenuated, and essentially unaffected by available magnetic fields. The characteristic attenuation length is given by the normal skin effect, $\delta = c/(2\pi\sigma\omega\mu)^{1/2}$.[1] For pure metals the electronic mean free path λ and electrical conductivity σ increase at low temperatures, and for a given frequency a temperature will eventually be reached where $\lambda > \delta$. Below this temperature the transmission of the microwaves must be described in terms of a nonlocal conductivity, and this regime is termed the anomalous skin effect.[2] When the temperature is lowered still further, the electronic collision time τ may continue to increase such that the condition $\omega_c\tau > 1$ will be realized for values of applied magnetic fields which are readily available in the laboratory (here ω_c is the cyclotron resonance frequency). When $\omega_c\tau \gg 1$ one finds that the spectrum of the magnetic-field-dependent transmitted microwaves can be remarkably rich, encompassing many different modes. In this paper we shall present experimental results, and an analysis, of three modes of magnetic-field-dependent microwave transmission through thin foils of pure alkali metals at cryogenic temperatures. The first of these modes has previously been studied via reflection spectroscopy, principally by Walsh and collaborators, and are termed cyclotron waves.[3,4] The second is a mode which we believe has not yet been reported in the literature, which we term "angular oscillations" because of their striking oscillatory dependence on the orientation of the applied magnetic field. The third mode relates to the field-dependent transmission when the dc field is oriented perpendicular to the sample surface. We identify these signals as the high-frequency Gantmakher-Kaner oscillations (GKO).[5]

As the Fermi surfaces of Na and K are very nearly spherical, we might expect that all the modes observed should be readily described by the electromagnetic response of a simple, degenerate, isotropic plasma. This point of view is probably qualitatively correct, and even reasonably quantitatively accurate, but only up to a point. The signal-to-noise ratio in these experiments is sufficiently large that it appears to be worth a detailed examination of the transmission signals to see if deviations from a simple free-electron model can be detected. One would like to be able to attribute these deviations to many-body effects, and thereby determine the coefficients pertaining to the Legendre polynomial expansion of the momentum part of the Landau correlation function.[6]

As we shall see, there are indeed significant deviations from the predictions of a free-electron model for the cyclotron waves, but there is a need for a better theoretical understanding of the boundary-value problem before an unambiguous interpretation in terms of many-body effects can be completed. This situation arises quite generally because the coupling to these modes is so large

that the problem must be treated self-consistently. This is in contrast to the case of coupling to the spin resonance mode, where the weak coupling allows a very satisfactory theoretical fit to be made to the observed spin-wave spectra, and coefficients pertaining to the spin part of the Landau correlation function can be readily deduced. An example of this latter type of data and analysis is in the preceding paper[7] and in Ref. 8. The effects of many-body interactions on the field normal signals are not known to a sufficient degree to warrant interpretation in terms of Landau coefficients. We shall show, however, that it is possible to utilize the measurements to determine v_F for particles moving along the magnetic field. Theoretical expressions for the angular oscillation signals are not known, even at the free-electron level, and it is our hope that the publishing of these data may stimulate work in this area.

Our experimental results for the cyclotron waves are compared with computations which make extensive use of the frequency- and wave-vector-dependent conductivity, $\sigma(k,\omega)$. The method of calculating σ including collisions, an external magnetic field, and Fermi-liquid effects, is discussed in the following paper by Fredkin and Wilson[9] (henceforth called FW).

II. EXPERIMENTAL PROCEDURES

The microwave spectrometer used in these experiments is one originally designed to study transmission electron spin resonance in metals.[10] The block diagram of the spectrometer is presented in Fig. 1. The sample forms the common wall between two microwave cavities which are tuned to the frequency of the spectrometer (typically between 9–10 GHz). Microwave power from a stable oscillator is amplitude modulated at an audio frequency and then coupled to match into the first, or transmit cavity (TC) thereby setting up a strong rf magnetic field at the surface of the sample. Although the rf field is in general strongly attenuated as it passes through the sample, under appropriate experimental circumstances a readily detectable amount of rf power is radiated from the far sample surface into the second, or receive cavity (RC). The receive cavity is in turn coupled to a sensitive superheterodyne receiver. As is shown in Fig. 1, some unmodulated power is taken from the main oscillator and combined with the modulated power coming from the receive cavity just prior to the receiver input. This reference power serves both to optimally bias the i.f. detector crystal, and also to allow tuning the spectrometer so as to be sensitive to the phase of the transmitted microwave fields as discussed in the next section. The phase shifter in the reference line allows one to adjust the relative phase of the reference and transmitted fields. The output of the i.f. detector is fed into a lock-in amplifier referenced to the audio modulation frequency. A maser preamplifier (not shown in Fig. 1) is also available, and when in use lowers the system noise temperature to ≈100 K (during operation at liquid-helium temperatures). Typically, the input power is 10^{-3} W, and the transmission signals may range from very strong at $\approx 10^{-14}$ W down to those detected with poor signal to noise at $\approx 10^{-19}$ W.

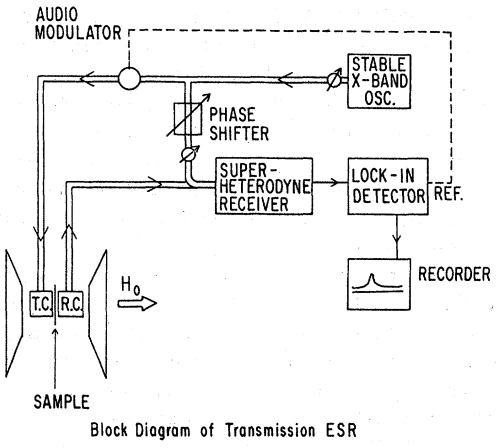

FIG. 1. Block diagram of the microwave transmission spectrometer. T. C. and R. C. are, respectively, the transmitting and receiving cavities.

All of the alkali metal samples were made by extruding the material through a slit slightly larger than the desired sample thickness and then squeezing it between thin glass plates for air-filled cavities or carefully prepared parafin coated dielectrid-filled cavities.[8] The samples were polycrystalline and are known to be strained at the operating temperatures.[7,8]

The cavities and sample are in a set of Dewars which allow the temperature to be set anywhere from 1.4 K to room temperature. The Dewars are in the gap of an electromagnet capable of producing dc magnetic fields up to 20 kG. The magnetic field can be oriented anywhere in the plane perpendicular to the rf magnetic field at the sample surface by rotating the magnet either manually or with a variable speed motorized drive. We have instrumented the magnet with an electronic angular readout that has resolution of better than 0.01°. Data is usually taken on an x-y recorder with the output of the lock-in amplifier on the y axis, and the x axis is either proportional to the magnitude of the dc field at fixed angle or vice versa.

In the following section there are many examples of data. The ordinates of the figures (in arbitrary

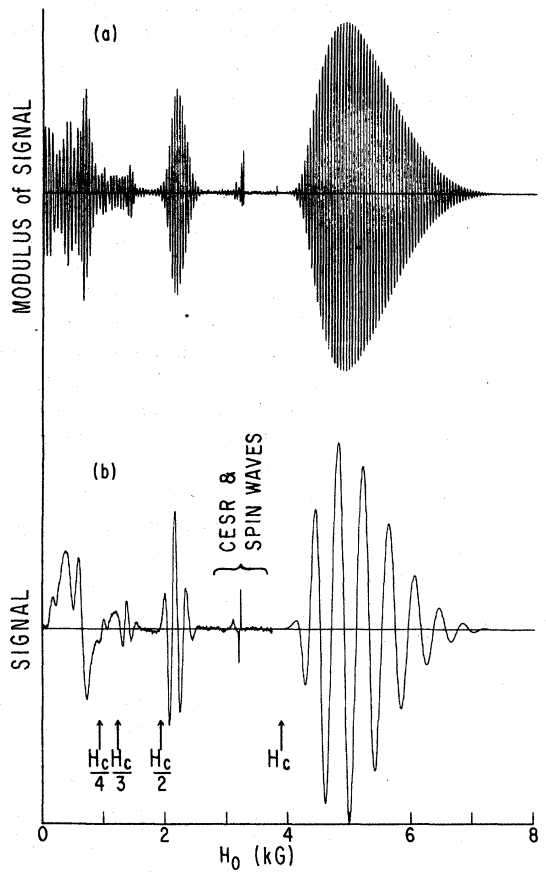

FIG. 2. Typical transmitted signals when the dc field is parallel to an alkali sample at cryogenic temperatures. The sample is a 0.0165-cm-thick Na slab at 1.3 K. The applied frequency is 9.19 GHz. The series of large broad peaks are the cyclotron wave modes. The CESR and associated spin waves are located between the fundamental and first subharmonic cyclotron wave modes as indicated. (Note: The gain was decreased by 22 dB above 4 kG.) (a) The reference phase is continuously and rapidly rotated during the sweep. The envelope of the rectified signal is proportional to the *modulus* of the transmitted microwave field. (b) The reference phase is held constant as the field is swept. The phase of the spectrometer has been set at a value which yields a symmetric CESR signal. (The CESR signal is severely time-constant limited for the sweep rates used and therefore appears comparable to the first spin wave.)

units) are labeled either "signal" or "signal modulus." We now define what is meant by these two terms. As was mentioned earlier, unmodulated reference power (or field) is added to the modulated power (or field) coming out of the receive cavity (which is in turn proportional to the field transmitted through the sample). The total field serves to bias the i.f. detector crystal into its linear range. As the reference field is much larger than the maximum transmitted field, the i.f. output is only sensitive to that component of the transmitted field which is in phase with the reference field. The quantity called signal is the output of the lock-in detector when tuned to the modulation frequency and is proportional to that component of the transmitted field which is in phase with a given reference field. Primary data are the dependence of the signal on either the magnitude or orientation of the dc magnetic field. Examples of such typical signals are Figs. 2(b) and 16(a), respectively.

In general, the variations in the signal as the dc field is swept reflects changes in both the amplitude and phase of the transmitted microwave field. The rapid oscillations of the signal above 4 kG as displayed in Fig. 2(b) correspond to successive changes in the phase by 2π. The milder variation of the overall envelope of the mode from 4 to 7 kG reflects the field dependence of the amplitude. By arranging to rotate the reference phase faster than the natural period of the signal oscillations, we obtain signals as displayed in Fig. 2(a), where the field dependence of the signal modulus, i.e., the rectified envelope, is more clearly visualized.

The procedure just described for obtaining the signal modulus, is not always practical (for example, if there were appreciable leakage of microwaves into the receiver).[11] An alternate procedure is to take one set of signal data for a particular value of the phase, and another set with the reference phase shifted by 90°. All that is required in this method is to be able to define the baseline, or zero of the field-dependent part of the signal. The modulus of these signals can then be computed as the square root of the sum of the squares. Examples of such computer manipulation of the signal data are presented in Sec. IIIA, for example (see Figs. 6 and 8). The initial phase is in principle arbitrary, but in practice we always use that

TABLE I. Values of m^*/m for the alkali metals.

	m^*/m
Na	1.24 ± 0.02[a]
K	1.217 ± 0.002[b,c]
Rb	1.22 ± 0.02[d,e]

[a] C. C. Grimes and A. F. Kip, Phys. Rev. 132, 1991 (1963).
[b] W. M. Walsh, Jr., L. W. Rupp, Jr., P. H. Schmidt, and R. N. Castellano, Bull. Am. Phys. Soc. 18, 336 (1973).
[c] A value deduced from an analysis of turning points in cyclotron waves resulted in $m^*/m = 1.210 \pm 0.006$, Ref. 24.
[d] B. Knecht, J. Low Temp. Phys. 21, 619 (1975).
[e] A value of 1.20 ± 0.02 has also been reported by C. C. Grimes, G. Adams, and P. H. Schmidt, Bull. Am. Phys. Soc. 12, Paper HG6 (1962).

which antisymmetrizes the conduction-electron spin resonance (CESR).

All the types of data discussed in this paper were taken on three alkali metals: Na, K, and Rb. In general, the best data were obtained at the lowest temperature, ≈1.4 K, and for the purest material as characterized by the resistivity ratio.[12] In Table I we present values of m^*/m used in our calculations.

III. DATA AND ANALYSIS

A. Cyclotron waves

When the magnetic field is oriented parallel to the surface of the sample several sets of oscillations are observed in the signal. These are illustrated in Fig. 2. As can be seen, there are field-dependent propagation "windows" starting at H_c, $H_c/2$, $H_c/3, \ldots$, where H_c is the field corresponding to cyclotron resonance. The conduction-electron spin resonance and associated spin-wave signals occur in the gap between the tail of the cyclotron wave window corresponding to $H_c/2$ and the onset of that at H_c. As can further be seen in Fig. 2, the main harmonic which starts at H_c reaches a peak at ≈5 kG and then dies out. We find no detectable field-dependent signal beyond ≈8 kG, and we believe this corresponds to a sufficiently high attenuation of the transmitted field that we regard any power emanating from the receive cavity at higher fields to be due to spurious leakage. However, if at any value up to ≈10 kG the magnetic field is rotated a few degrees away from field parallel, there is a dominant transmitted signal which we believe is a continuation of the cyclotron modes. Above 10 kG the nature of the transmission away from field parallel is quite different, and it is these signals that we have termed angular oscillations, and which are discussed in Sec. III B.

The cyclotron waves in metals were first identified by Walsh and Platzman.[13] They reported the observation of additional oscillations on the high-field side of Azbel-Kaner cyclotron resonance signals in pure potassium slabs. Subsequent detailed measurements have been interpreted by assuming that the oscillations correspond to discrete values of wave vector, given by $kL = n\pi$. They were able to analyze data taken at several frequencies in terms of a universal dispersion relation calculated for these modes assuming infinite $\omega\tau$. Small, but significant deviations at the onset, or small k-vector end, of the relation were then interpreted as being due to many-body effects.[3] Their best values of the Landau parameters for K, which they denote by A_n (often called F_n in the literature) are: $A_2 = -0.022 \pm 0.002$, $A_{n>2} < 0.003$.[14]

After it was realized that the oscillatory strong signals seen in transmission below and above the region of spin resonance were also due to the cyclotron waves, we were motivated to attempt a similar analysis. Considerable advantages might be expected; the signal-to-noise ratio is significantly better in transmission then reflection, the Azbel-Kaner response is completely attenuated so the oscillations of interest are on a straight baseline, and the method of excitation and detection are unambiguously defined. (The latter point is in contrast to the way the reflection experiments had to be performed, in practice, to obtain adequate signals.[13]) It was soon realized that this direct approach was not applicable for reasons which will be discussed in detail, and as a consequence it was felt that quantitative measurements would only be possible if there was an appropriate theoretical formulation of the boundary value problem so as to allow precise comparisons of the total line shape. Our efforts to interpret the observed spectra in terms of proposed solutions to the boundary value problems constitute the thrust of the rest of this section. Some theoretical aspects of the boundary value problems and the formulas used by us as possible solutions are discussed in the following paper.[9]

In Fig. 3 we present the infinite-$\omega\tau$ free-electron dispersion relations for the fundamental cyclotron mode and the first subharmonic when the rf electric field is parallel to the dc field.[15] All the data and analysis in this article are for this condition (the ordinary wave) although we have also observed the analogous cyclotron waves in transmission for the other polarization (the extraordinary wave). Note that the dispersion relations become multivalued at higher ω_c/ω. Thus, one may expect some complications in terms of multiple ex-

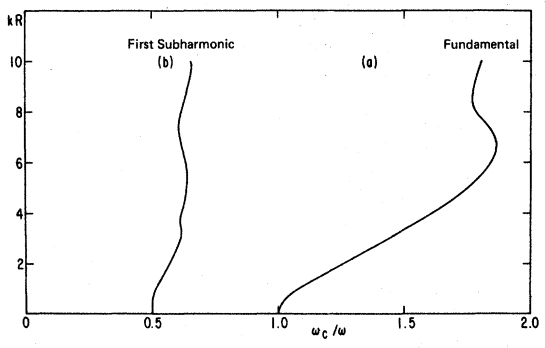

FIG. 3. Infinite $\omega\tau$, free-electron dispersion relations for the cyclotron waves when the rf electric field is parallel to the dc magnetic field. R is the cyclotron radius at cyclotron resonance. (a) Fundamental. (b) First subharmonic.

citations beyond $\omega_c/\omega \sim 1.7$ for the main mode, and $\omega_c/\omega \approx 0.6$ for the first subharmonic. Dunifer *et al.*[16] have identified anomalies in the reflection spectra with the turning points. In Fig. 3 the ordinate is made dimensionless by scaling with R, the cyclotron radius at cyclotron resonance.

A detailed discussion of the calculation of the dielectric tensor appropriate for the cyclotron waves is presented by Platzman and Wolff.[4] There is also a discussion of the boundary value problem in a metal. For reasons next discussed, it was necessary in our work to be able to include the effects of a finite τ and to try to incorporate true line-shape solutions. The effects of a finite $\omega\tau$ on cyclotron-wave propagation in metals at long wavelengths, and calculation of the dispersion curves (without Fermi-liquid effects) have been discussed by Fransden and Gordon.[17] In what follows we analyze our data incorporating dispersion curves which include both finite $\omega\tau$ and Fermi-liquid effects. All the dispersion relations and related formulas used for comparison with our data as presented in the rest of this section were calculated according to algorithms provided by FW, as discussed in the following paper.[9]

The wave vector $k = k_r + ik_i$ of the dispersion relations in Figs. 3(a) and 3(b) is pure real and describes the change in phase of a cyclotron wave propagating in the z direction (taken as the normal to the plane of the rf and dc magnetic fields). It is understood that since τ is infinite the imaginary part of the wave vector, k_i, is zero, within the mode "window" from $\omega_c/\omega = 1$ to ≈ 1.86. Beyond either edge of the window k_i increases precipitously. The effects of finite Landau coefficients A_2 and A_3 on the infinite $\omega\tau$ dispersion relation for the fundamental mode are illustrated in Fig. 4. It can be seen that A_2 primarily shifts the onset of the window from $\omega_c/\omega = 1$, and A_3 changes the slope of the linear region of the curve. (For the range of kR considered in this work, A_0 and A_1 have negligible effect on the dispersion relation.[4]) Thus, it might appear that by simply observing the field at which there is a sharp onset of transmitted power one could find the deviation from H_c, and hence know A_2 directly. The trouble with this procedure in practice is that although $\omega\tau$ is reasonably high for our samples, typically between 15 and 50, it is not yet high enough. We can observe transmitted power for many samples both below and above the infinite $\omega\tau$ window limits. Furthermore, the signals are essentially exponentially attenuated, and it is difficult to define an "onset field" to an accuracy necessary to determine the small deviations expected due to the finite A_2 effects. In Figs. 5(a) and 5(b) we present the real and imaginary parts of the complex dispersion relations for the

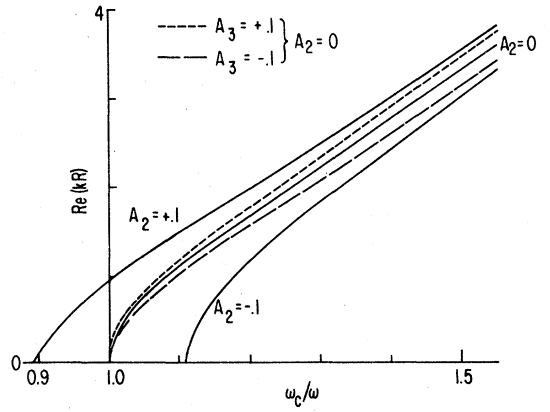

FIG. 4. Infinite $\omega\tau$ dispersion relation for the cyclotron wave in the vicinity of the fundamental mode for illustrative values of the Landau coefficients A_2 and A_3. A_3 is zero unless noted. The curve for $A_2 = 0$ is the same as part (a) of Fig. 3. We note that A_2 predominantly shifts the onset of the dispersion relation, and that A_3 changes the slope in the linear region.

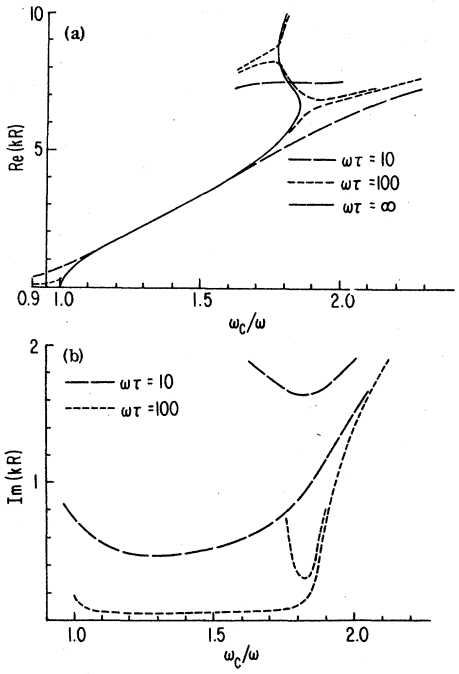

FIG. 5. Real (a) and imaginary (b) parts of the complex dispersion relation in the region of the fundamental mode for several values of $\omega\tau$. We note the following features. (i) For finite $\omega\tau$, the real part of k does not have a sharp onset at $\omega_c/\omega = 1$, but is spread out and can extend well below. (ii) Although the damping (i.e., imaginary part of k) increases rapidly when $\omega_c/\omega < 1$, one can readily expect transmission in that region for finite $\omega\tau$. (iii) In the region of the turning point, $\omega_c/\omega \approx 1.8$, the dispersion relation becomes multivalued in a complicated manner. Nonetheless, the entire set of branches is included in our line-shape calculations.

free-electron theory, but with several finite values of $\omega\tau$. The extension of a finite propagation region significantly beyond the infinite $\omega\tau$ window region in both directions is evident.

As noted earlier, the many oscillations of the signal in a typical spectrum such as Fig. 2(b) are predominantly due to the $k_r L$ evolving through successive multiples of 2π. As can be seen in Fig. 5(a), the dispersion relation is quite linear, and also independent of $\omega\tau$ for a significant fraction of the window, say from $1.2 \leq \omega_c/\omega \leq 1.6$. As discussed in Sec. IV B 2 a of the preceding paper,[7] it is found empirically that a plot of the zero crossings of the cyclotron wave signals versus magnetic field results in a good straight line relationship over the major part of the spectrum. (See Fig. 9 of the preceding paper.) It is also found that the slope is proportional to the sample thickness and is independent of $\omega\tau$ (as varied by warming the sample). Thus, one expects that whatever the precise formula describing the transmitted field h_t may be, a major part must be a term of the form e^{ikL}. However, an attempt at a quantitative fit of the modulus of the signal to $|e^{ikL}|$ fails badly. (See Fig. 6.) Further, since we are interested in obtaining information about the Landau coefficients, and as we have noted in Fig. 4, a finite A_2 mainly shifts the onset and has very little effect on the slope in the linear region, we are most interested in being able to make a qualitative fit between the experiments and some appropriate theoretical relation at small k, i.e., near the onset.

As discussed in FW, an "honest" calculation of the boundary value problem, assuming an imposed current sheet set up by the driving fields, results in h_t being proportional to e^{ikL}/k. Although this expression for h_t fits the data much better than e^{ikL} alone, there are still very substantial deviations (see Fig. 6). We were, therefore, led to try an alternate formulation as discussed next.

In the course of much agonizing over the appropriate formulation of the boundary value problem, various approaches were suggested to us by Fredkin and Wilson. One of these is that h_t should be taken as

$$h_t \propto e^{ikz} \frac{\partial \sigma}{\partial k}, \tag{1}$$

where $\sigma(k, \omega)$ is the conductivity. The present justification for our use of this expression is that it reduces to the "honest" calculation for small k values, and that as we shall see, it looks like it fits the overall data significantly better. In some cases it fits so well that one is inclined to believe that when the appropriate derivation is discovered it will result in an expression very close to this one. In any event, in Fig. 6 we have

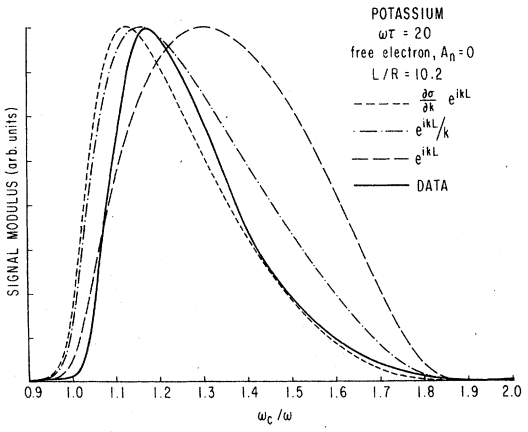

FIG. 6. Comparison of the signal-modulus data of the fundamental cyclotron mode for a potassium sample at 1.4 K (solid curve), with curves calculated for several theoretical expressions as discussed in the text. L/R is the thickness of the sample expressed in units of the cyclotron radius at cyclotron resonance. The frequency was 9.74 GHz. All of the theoretical curves are for all $A_n = 0$, i.e., free-electron theory. The data curve represents the result of combining in quadrature two signals taken with their reference fields 90° apart as discussed in the definition of signal and signal-modulus in Sec. II.

presented a comparison of the fundamental signal modulus for a potassium sample with the computations for $|h_t|$ using Eq. (1), e^{ikL}/k, and e^{ikL}. Equation (1) comes closest to fitting the data, except that it appears translated by a small amount. This suggests we should incorporate a finite A_2 which, as we have seen in Fig. 4, predominantly shifts the dispersion relation. A "best" fit is obtained by adjusting the variables A_2 and τ in the manner next described.

To fit the data we first compare the modulus of the signal for the fundamental with the results of Eq. (1), calculated for the free-electron theory and with a finite value of $\omega\tau$. Varying $\omega\tau$ over the region of interest does not appreciably change the width, peak position, or nature of the modulus of the signal, although it does affect the slope of the leading and trailing edges. We chose to focus our primary fit on the leading edge for the reasons discussed. As can be seen in Fig. 6, following an appropriate choice of $\omega\tau$, the data and calculated values for Eq. (1) are quite similar, but shifted by a small amount. Next, one estimates a trial value of A_2 from the separation of the leading edges in Fig. 6, and we get the results shown in Fig. 7. (Actually, the fit shown is the result of several iterations between A_2 and $\omega\tau$.) Although the computations for Figs. 6 and 7 were done with values selected to give the best fit for Eq. (1), we should emphasize that we have found that it is

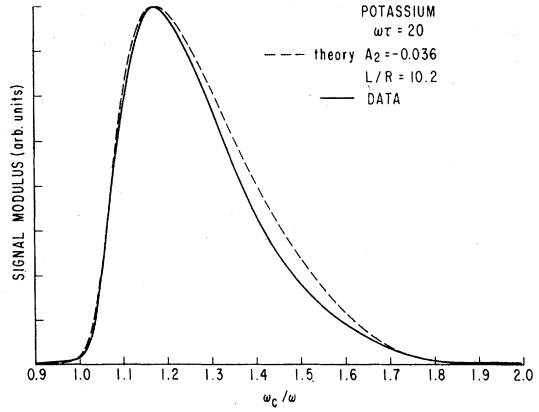

FIG. 7. Comparison of the signal-modulus data of the fundamental cyclotron mode for a potassium sample at 1.4 K (solid curve) with a curve as calculated for Eq. (1) and incorporating values of A_2 and $\omega\tau$ so as to give a best fit to the leading edge. The frequency was 9.742 GHz.

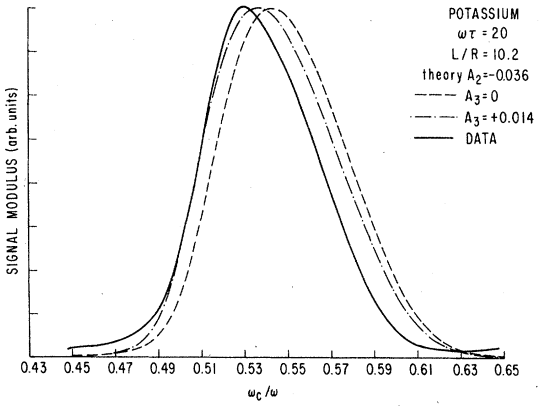

FIG. 8. Comparison of the signal-modulus data of the first subharmonic cyclotron mode for a potassium sample at 1.4 K, with curves calculated using Eq. (1), with $A_3 = 0$ and $A_3 = 0.014$. The latter value corresponds to the best fit to the leading edge. The value of A_2 in both cases was that deduced from the analysis, as illustrated in Fig. 7. The frequency was 9.742 GHz.

not possible to make the other two expressions fit as closely to the trailing edge of the data, once the leading edge is fit.

Having obtained values for $\omega\tau$ and A_2 from the fit to the modulus of the fundamental signal, we are interested in continuing the process to possibly extract values for A_3. Although in principle A_3 would affect the fit to the trailing edge, in practice this is not significant, and we instead turn to looking at the modulus of the first subharmonic signal. To a first approximation A_3 shifts the onset at the first subharmonic similarly to the way A_2 shifts the onset for the fundamental. In Fig. 8 we compare the first subharmonic modulus data with the results of Eq. (1) using the same $\omega\tau$ and A_2 values which gave the best fit, as illustrated in Fig. 7. We see that the overall fit is still quite good, but that there could be some improvement by incorporating a small A_3. The final best fit corresponding to an A_3 of +0.014 is also shown in Fig. 8. To summarize the data-fitting procedure to this point we may conclude that values for $\omega\tau$, A_2, and A_3 are obtained from the fundamental and first subharmonic modulus data.

We may also compare Eq. (1) to the data taken at a fixed reference phase, i.e., the signal. To do this we must identify the appropriate reference phase angles that correspond to the way the signal traces are taken. (As was discussed the CESR signal is antisymmetrized and then two sets of data are taken, one at that phase, and another 90° removed.) Neither the real nor the imaginary parts of Eq. (1) turn out to be close to the appropriate phases for matching the experimental signal traces referenced to a CESR symmetric or antisymmetric signal. We can systematically vary the reference phase (on the computer) to get a best fit, and in Fig. 9 we present a typical result of such a procedure. For this case the reference phase experimentally corresponds to an antisymmetric CESR signal, and the phase shift relative to the real part of Eq. (1), $\Delta\phi_c$, was 45°. Although the overall fit is quite impressive, we do note that the

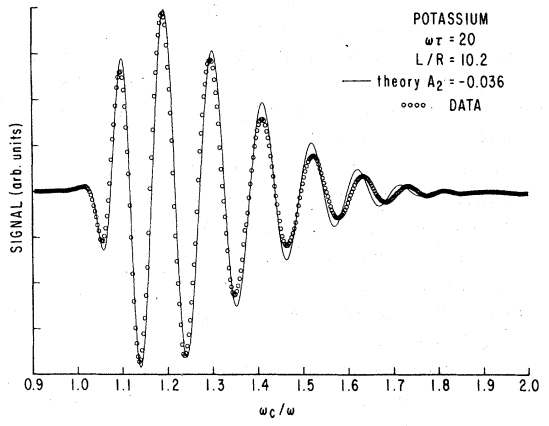

FIG. 9. Comparison of the signal data (dots) of the fundamental cyclotron mode for a potassium sample at 1.4 K with a curve calculated using Eq. (1) and the values of $\omega\tau$ and A_2 as deduced from the signal-modulus analysis. The frequency was 9.742 GHz, with the experimental reference phase corresponding to an antisymmetric CESR signal. The computational reference phase was varied systematically until a best fit to the first oscillation was obtained, which, in this case, is 45° from the real part of Eq. (1).

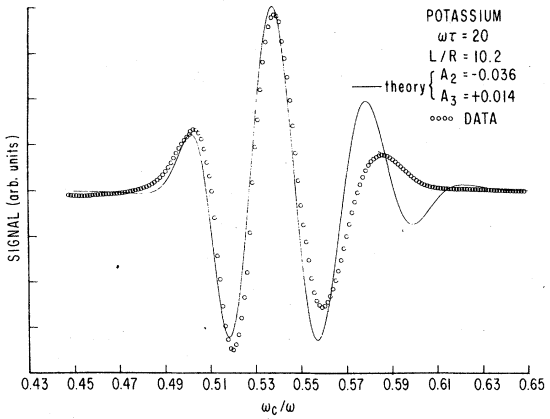

FIG. 10. Comparison of the signal data (dots) of the first subharmonic cyclotron wave for a potassium sample at 1.4° with a curve as calculated using Eq. (1) and the values of $\omega\tau$, A_2, and A_3, as deduced from the signal-modulus analysis. The frequency was 9.742 GHz, and the experimental reference phase corresponded to an antisymmetric CESR signal. The computational reference phase was varied systematically until a best fit to the first oscillation was obtained, which, in this case, is 117° from the real part of Eq. (1).

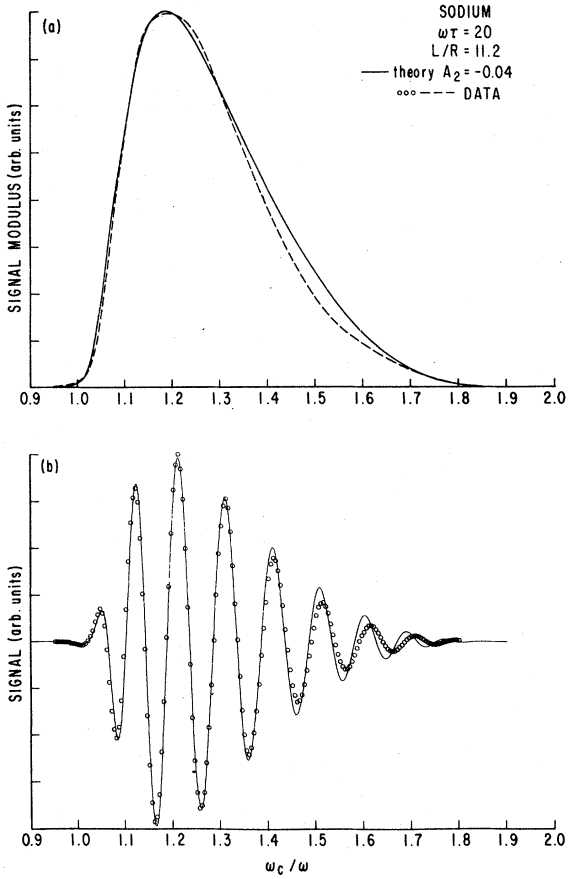

FIG. 11. (a) Comparison of the signal-modulus data of the fundamental cyclotron mode for a sodium sample at 1.4 K with a curve as calculated using Eq. (1) and where $\omega\tau$ and A_2 have been chosen to give a best fit to the leading edge. The frequency was 9.2 GHz. (b) Comparison of the signal data of the fundamental cyclotron mode for the same sample as (a), with a curve calculated using Eq. (1) and the values of $\omega\tau$ and A_2 as chosen by the fit of (a). The experimental reference phase corresponded to an antisymmetric CESR signal. The computational reference phase was varied systematically until a best fit to the first oscillation was obtained, which in this case is −118° from the real part of Eq. (1).

theory and data begin to deviate at the highest fields. We expect some discrepancies in the magnitude of the peaks, since, as can be seen from Fig. 7, we do not get a perfect fit to the modulus at the trailing edge. This seems to be an inherent failure of Eq. (1). Additionally, as seen in Fig. 9, the data and theory are getting noticeably out of phase for $\omega_c/\omega > 1.5$. However, we must recall that the phase change is determined by both k_r and L. We could get a better fit to the data in Fig. 9 if either L were decreased by $\cong 2\%$, or if an $A_3 \cong 0.05$ were introduced. If such a large A_3 were used, however, it would change the fit of the first subharmonic illustrated in Fig. 8. Thus, we seek another explanation. Aside from the fact that there could be an error of about 1% in our assigned value of L, we should point out that since we do not have a detailed microscopic solution to the boundary value problem, one has to even be cautious as to what parameter is ascribed to the correct "thickness" of the sample. It might be that the appropriate thickness should not be the physical one, but rather modified by some appropriate fraction of the cyclotron radius. Further, the fact that $\Delta\phi_c$ is not zero, and varies from sample to sample, suggests we are missing some additional term in Eq. (1). At the least, this term contains a constant phase shift; at the worst, it could be field dependent. Evidence that this may be so comes from the subharmonics. The data taken with a constant phase reference for the first subharmonic can also be compared with Eq. (1), and this is presented in Fig. 10. The best fit now requires $\Delta\phi_c = 117°$. We have no current explanation for this additional field dependence of the phase.

Typical data illustrating the analogous final fit for a Na sample are presented in Figs. 11 and 12 for the fundamental and first subharmonic, respectively. We again note the development of a phase difference between the data and theory at higher values of ω_c/ω. In Fig. 13 we present typical data and computational fit for the fundamental cyclotron mode for a Rb sample. As noted in the

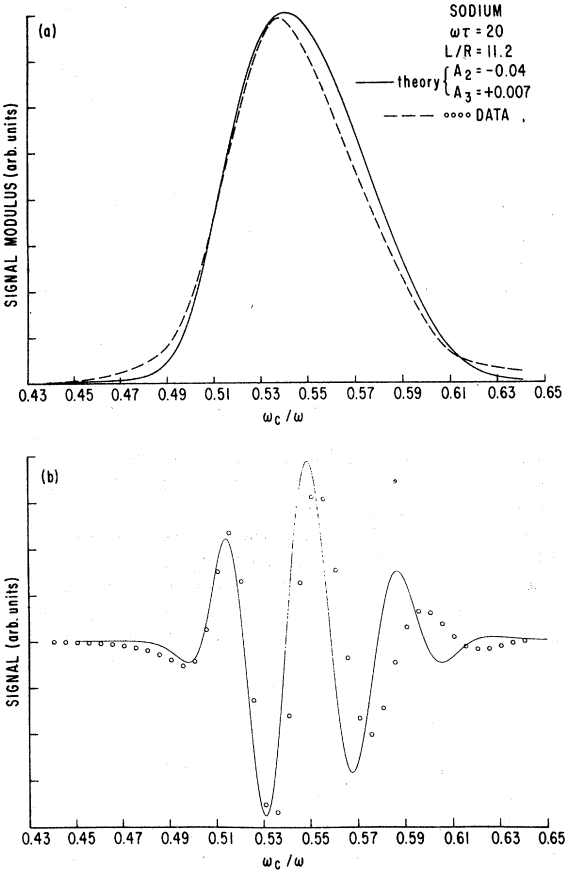

FIG. 12. (a) Comparison of the signal-modulus data of the first subharmonic cyclotron mode for a sodium sample at 1.4 K with a curve calculated using Eq. (1) $\omega\tau$ and A_2 were chosen from the signal-modulus fit of Fig. 11 (a), and A_3 is chosen to give the best fit to the leading edge. The frequency was 9.2 GHz. (b) Comparison of the signal data for the first subharmonic cyclotron mode for the same sample as (a), with a curve calculated using Eq. (1) and values of A_2 and A_3 as deduced from the signal-modulus analysis. The experimental reference phase corresponded to an antisymmetric CESR signal. The computational reference phase was varied systematically until a best fit for the first oscillation was obtained, which in this case, is $-99°$ from the real part of Eq. (1).

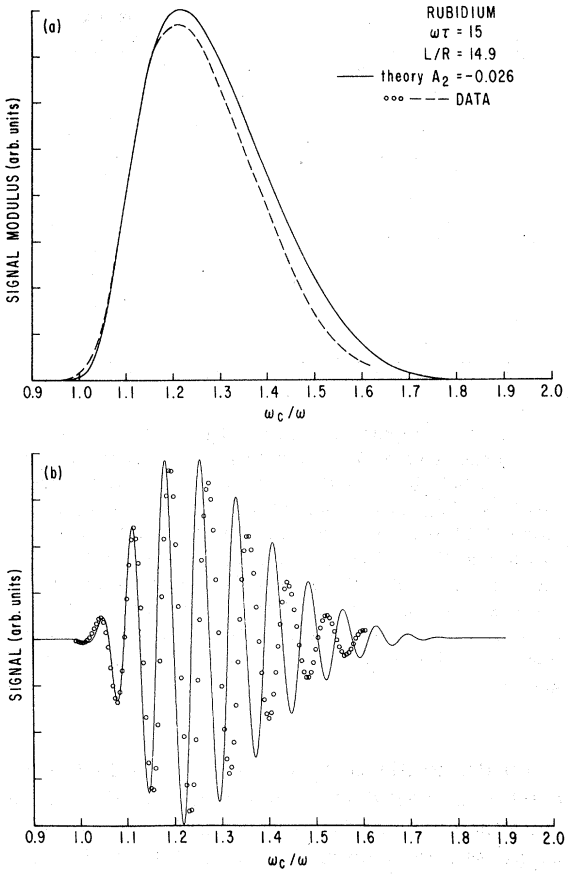

FIG. 13. (a) Comparison of the signal-modulus of the fundamental cyclotron mode for a rubidium sample at 1.4 K with a curve as calculated using Eq. (1) and where $\omega\tau$ and A_2 have been chosen to give a best fit to the leading edge. The frequency was 9.2 GHz. (Due to the process of reconstructing the signal modulus from the two phase signal data, the curves are not perfectly normalized at the maximum amplitude. This does not appreciably change the results for the data fit.) (b) Comparison of the signal data of a fundamental cyclotron mode for the same sample as (a), with a curve calculated using Eq. (1) and the values of $\omega\tau$ and A_2 as chosen in (a). The experimental reference phase corresponded to an antisymmetric CESR signal. The computational reference phase was varied systematically until a best fit to the first oscillation was obtained, which, in this case, was $-1°$ from the real part of Eq. (1). Note the appreciable deviation in phase between theory and experiment at higher values ω_c/ω.

figure, we have used an L/R value of 14.9 corresponding to our best estimate of the physical thickness of the sample. As is seen in Fig. 13(b), the theory and data are very significantly out of phase at higher ω_c/ω values. In Fig. 14 we present the same data compared with the calculations when L/R has been set at 13.8 in order to obtain a good fit. We do not believe a change of this magnitude can be attributed to either an error in the thickness measurement (corresponding to $\approx 7\%$) or a very large A_3 (≈ 0.2), but it does illustrate the need for determining these parameters independently and as accurately as possible, as well as the need for further refinement in Eq. (1), at least insofar as phase is concerned. Unfortunately, the signal-to-noise ratio at the first subharmonic was not sufficiently high for the Rb samples to warrant an attempt at data fitting.

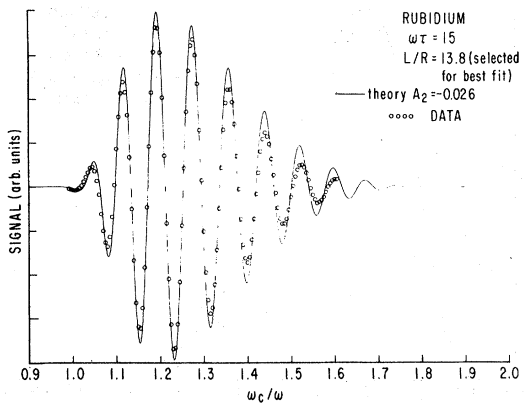

FIG. 14. Comparison between the signal data for the same conditions as Fig. 13 with a curve calculated as in Fig. 13(b), but with the L/R value set at 13.8. Note that by making this change (from the experimental value of 14.9) we achieve a significantly better fit to the data at the higher values of ω_c/ω. As discussed in the text, it is not believed that the thickness measurement is in error, but that these data indicate that the correct description of the cyclotron waves in rubidium may be more complicated than that for potassium or sodium.

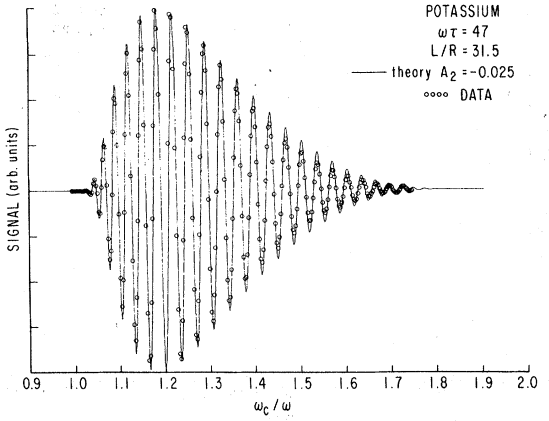

FIG. 15. Canonical illustration of the quality of fit possible between theory and experiment for the fundamental cyclotron-wave signal in a potassium sample. This sample is at 1.4 K, and the applied frequency 9.731 GHz. A_2 and τ are the primary adjustable parameters. The experimental reference phase corresponded to an antisymmetric CESR signal. The computational reference phase was varied systematically until a best fit to the first oscillation was obtained, which in this case is 18° from the real part of Eq. (1).

In order to illustrate why the authors feel there must be a great deal of significance to Eq. (1), despite the evidence for deviations just discussed, we present the data and theoretical fit of Fig. 15. While it is admittedly our cononical example of a best fit, when one considers the quality of this fit in terms of the complex dispersion curve, modified by the A_2 coefficient and $\omega\tau$ as the only ad-

TABLE II. Results of cyclotron-wave analysis.

Sample	Harmonic F: fundamental S: first subharmonic	Frequency (GHz)	L/R	$\omega\tau$	Present work A_2	Present work A_3	Other work
Potassium							
V	F	9.7	10.2	20	-0.036		$A_2 = -0.022 \pm 0.002$[a]; $\lvert A_n\rvert < 0.002$, $n > 2$
V	S	9.7	10.2	20		+0.014	
Z	F	9.7	31.5	47	-0.025		
	S	9.7	31.5	47		+0.015	
Sodium							
P	F	9.2	11.2	20	-0.04		$A_2 \cong -0.05 \pm 0.02$[b]; $\lvert A_3\rvert < 0.02$
	S	9.2	11.2	20		+0.007	
$Z2$	F	9.2	4.4	15	-0.04		
H	F	9.2	12.5	9	-0.05		
ZY	F	9.2	14.6	25	-0.037		
Rubidium							
5	F	9.2	13.8	10	-0.026		
7	F	9.2	14.9	15	-0.026		

[a] W. M. Walsh, Jr., L. W. Rupp, Jr., P. H. Schmidt, and R. N. Castellano, Bull. Am. Phys. Soc. 18, 336 (1973).

[b] Reference 4, page 250.

justable parameters, one cannot help feeling that there must be a physical justification for Eq. (1).

How reliable then are these A_n coefficients? We remind the reader that it is the signal *modulus* data that was used to fit the A_n. Hence if the $\Delta\phi_c$ term arises from a multiplicative factor, it will not matter. We suggest that further refinements in the data-fitting procedures are not warranted given the present state of the theory. Our results for the A_2 and A_3 coefficients are summarized in Table II, where they can be compared with those of Walsh *et al.* For Na and K, where the Fermi surfaces are known to be very spherical, we believe the A_2 coefficients are meaningful. We note that there appears to be good agreement with the values obtained by Walsh and co-workers via reflection spectroscopy,[4,14] although, as we mentioned earlier, we do not understand why their procedure of fitting the infinite $\omega\tau$ dispersion relation should be justified. The A_3 are sufficiently close to zero, compared to the relevant errors, that one cannot draw any conclusions other than that they are smaller than A_2.

There are at least two potential sources of systematic error in these determinations of the A_2 coefficients. The first is quite simple. We are basically measuring the deviations from the field at cyclotron resonance. However, this field is only known with an accuracy to which m^* is known. We have used the values of m^* as listed in Table I, but any change in these values changes A_2 correspondingly. The second consideration is the potential effects of anisotropy of the Fermi surface. Freedman and Fredkin have considered this question[18] and have shown that simple cubic distortion would result in deviations of the onset for these modes, and hence might mask the true many-body contributions. The Fermi surfaces for Na and K are sufficiently spherical that this effect is probably not important, but the situation for Rb is uncertain.

B. Angular oscillations

Figure 16(a) shows the transmission signal for a 0.018-cm-thick sample of Na as a function of magnet angle for a constant field strength of 13 kG at 9.155 GHz. The data are taken at 1.4 K. θ is the angle between the magnetic field and the sample surface. Beyond $\theta = 40°$ there is some transmission all the way to $\theta = 90°$, but it does not have a comparable angular dependence and appears qualitatively different. We note that the angular dependence separates into two characteristic sets of oscillations, one between 0 and 10°, and the other between 10 and 40°. We refer to these as type A and B, respectively. The oscillations in Fig. 16(a) are due to an angular dependence of the phase. Their modulus would correspond to the rectified envelope.

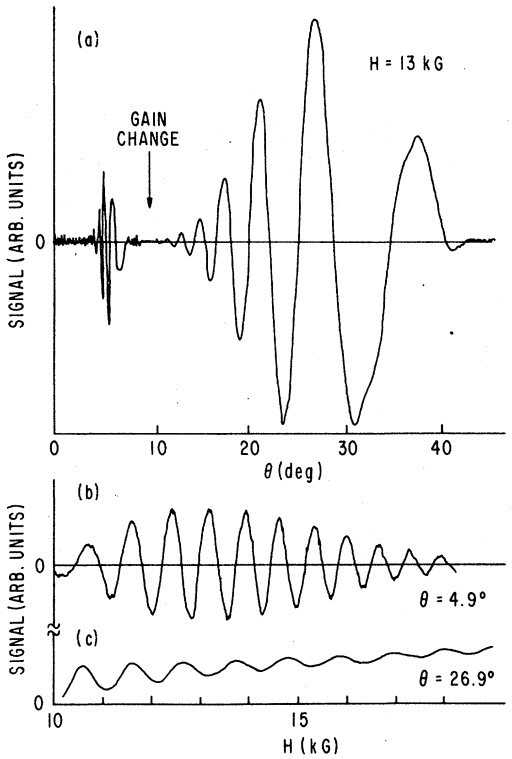

FIG. 16. (a) Transmission signal for a 0.017-cm-thick sodium sample as a function of θ, the angle between the dc magnetic field and the surface. The field was held constant at 13 kG. The temperature was 1.4 K, and the applied frequency 9.155 GHz. The gain was decreased 22 dB for angles greater than $\approx 9°$. There is clearly a qualitative difference to the set of oscillations below 10° as compared to those above. We have termed these two sets the A and B modes, respectively. (b) The magnetic field dependence of the signal for $\theta = 4.9°$, corresponding to the center of the A-mode oscillations. The rapid oscillations are attributed to a phase dependence on the magnetic field. The amplitude dependence is given by the rectified envelope. (c) The magnetic field dependence of the signal for $\theta = 26.9°$, corresponding to the center of the B-mode oscillations. The signal corresponds to a slowly decaying set of phase oscillations riding on a background that increases with field.

The two angular modes show different behavior when the magnetic field is swept while its orientation is held constant. In Fig. 16(b) we present the signal when the magnetic field is swept while oriented at $\theta = 4.9°$, which corresponds to the center of the A mode. These are again phase oscillations with the amplitude dependence given by the (rectified) envelope. In one sample of very

pure potassium there appears to be interference between two sets of oscillations in the field sweeps. If the sweep is continued lower in field, there is a region of very low transmission until one arrives at the tail of the cyclotron waves. Figure 16(c) shows the field dependence of the signal at $\theta = 26.9°$, which is in the center of the B mode. It consists of some decaying phase oscillations riding on a background that increases with field. If the sweep is continued to lower field, we find that these these oscillations appear to be a continuation of the $\theta \neq 0$ cyclotron waves mentioned above. Our interpretation of the data in Fig. 16(c) is that the oscillations are due to a decaying tail of the $\theta \neq 0$ cyclotron waves and are superimposed on a new signal that increases with increasing field and whose phase is independent of field. The type-B signals of Fig. 16(a) are attributed to the nonoscillatory component of the data shown in Fig. 16(c).

The type-B signals behave like a mode discussed by Konstantinov and Skobov.[19] They suggest that there should be a mode whose phase is independent of magnetic field but which depends on the angle θ and sample thickness as

$$\varphi = L\omega/v_F \sin\theta, \tag{2}$$

where φ is the phase of the transmitted field (to within an additive constant), L is the sample thickness, and θ the angle between the magnet field and the sample surface. This formula has a simple intuitive origin as discussed by Sparlin.[20] $L/\sin\theta$ is the path length across the sample parallel to the magnetic field. Dividing this by v_F gives the time it takes on electron traveling parallel to the field to cross the sample. Multiplying by ω gives the phase shift of the current carried by these electrons relative to the driving rf field. In Fig. 17 we compare angular sweeps for two values of the magnetic field (and the same spectrometer phase setting). We see that the locations of the zero crossings, and thus the phase, is independent of field strength. By increasing the temperature we have verified that decreasing τ does not affect the location of the oscillations although it does reduce the amplitude.

Figure 18 is a graph of the relative phase of the type-B signal (in units of 2π) versus $1/\sin\theta$ for a sample of Rb. The fit to a straight line is excellent, verifying the $1/\sin\theta$ hypothesis. We have attempted a quantitative fit to the slope of these data. Using the value of $v_F = \hbar k_F/m^*$, with m^* from Table I, we find that for Na the thickness as determined from the slope agrees with that measured directly, or, in a second case inferred from spin wave measurements, to within 0.5%. Unfortunately, we were not able to make a similar comparison for K because the high-resolution angular

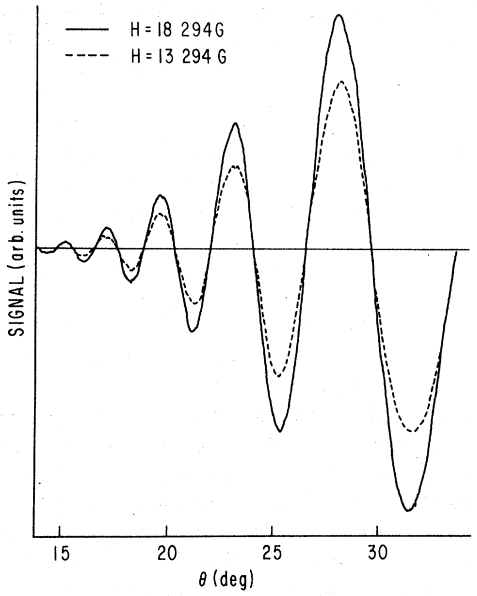

FIG. 17. B-mode oscillations as a function of θ for two values of the dc field (and with the same reference phase setting). We note that although the signal is stronger at higher field, the positions of the peaks and zero crossings is unchanged. The sample was rubidium, 0.017 cm thick, at a temperature of 1.4 K. The frequency was 9.2 GHz.

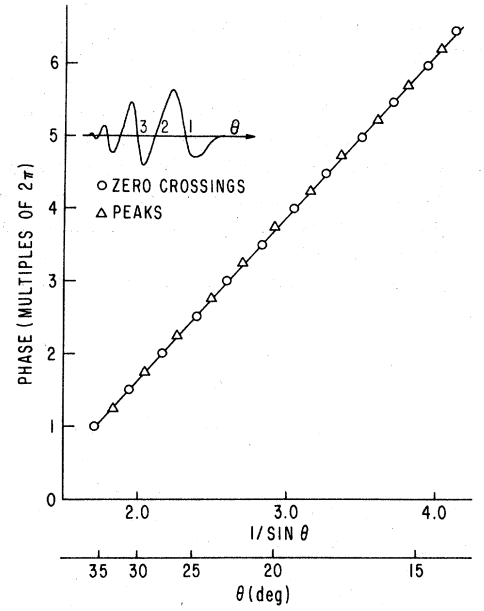

FIG. 18. Relative phase of the type-B mode oscillations as a function of $1/\sin\theta$. θ is the angle of the magnetic field relative to the surface of the sample. The inset indicates the numbering scheme for the zero crossings. The sample was rubidium 0.017 cm thick at 1.4 K. The frequency was 9.2 GHz.

readout system was not available at the time the highest-purity K samples were being run. (We find agreement to only 4%, but that is within the estimated error.)

The situation for Rb appears to be different. While the data plotted in Fig. 18 support the $1/\sin\theta$ dependence of Eq. (2), the thickness calculated from the slope is about 6% thinner than that measured directly. As will be discussed in Sec. III C, the GKO in Rb also do not agree with the theoretical expressions as closely as they do in Na and K, and we have seen a comparable disagreement in the fit to the cyclotron data of Sec. III A, i.e., Fig. 13(b). These may be due to effects of strain or the larger nonsphericity of the Rb Fermi surface.[21] Alternatively, since we know the thickness one can look upon these data as a measurement of some appropriate average Fermi velocity in Rb.

We have observed similar angular oscillations in aluminum, and since all of the other modes discussed, plus the spin waves, have been observed in Cs, expect that they are present there as well.

The type-A signals can only be detected in our highest $\omega\tau$ samples. In Fig. 19 we plot the phase dependence of the signal as a function of θ for several values of the magnetic field. The data are from a sample of Na with an $\omega\tau \approx 60$, as determined by fitting the linewidth of the first spin wave. One should not attempt to infer the phase dependence as a function of magnetic field from Fig. 19, as each curve has been drawn with an arbitrary additive constant for ease of presentation. The progress along any one curve gives the phase shift as a function of angle. The inset to Fig. 19 is a typical high-resolution angular sweep at constant field.

In Fig. 20 we present the relative phase of the transmission signals for the type-A mode as a function of the magnetic field for several magnet angles. The relative positions of the curves are meaningful but the absolute phase is correct only up to an arbitrary additive constant. Figure 19 can be used to interpolate for angles between these shown. The lines begin and end where the signal is just detectable above the noise, although at the smaller angles our field limit of 20 kG kept us from seeing the high-field end of the mode.

We have not been able to identify the type-A signals with any theoretical model. The data in Fig. 19 were suggestive of a Doppler-shifted cyclotron mode (DSCM),[22] since the phase changes

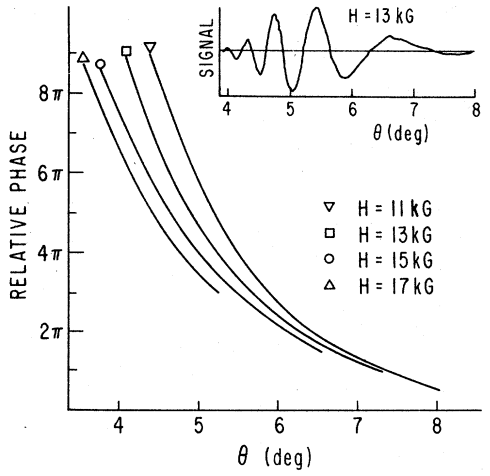

FIG. 19. Relative phase of the type-A mode oscillations as a function of θ, the angle of the magnetic field relative to the surface of the sample, for several values of the field. The progress along any one curve gives the phase shift as a function of angle. One should not attempt to infer the phase dependence as a function of magnetic field from these data, as each curve has been drawn with an arbitrary additive constant for ease of presentation. The inset is a typical high-resolution angular sweep at constant field. The data are for a sodium sample 0.017 cm thick at 1.4 K. The frequency was 9.2 GHz.

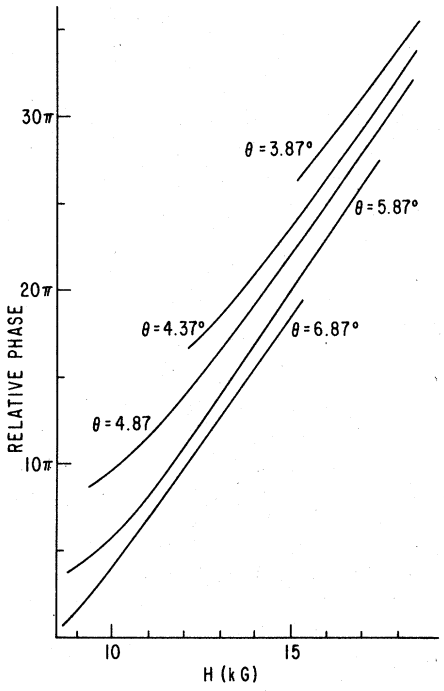

FIG. 20. Relative phase of the signal for the type-A mode oscillations as a function of magnetic field for several magnet angles θ. The relative positions of the curves are meaningful, but the absolute phase is arbitrary. The data of Fig. 19 can be used to interpolate for angles between those shown. The lines begin and end where the signal is either just detectable, or where we reached the limit of our magnet (20 kG). The sample was sodium 0.017 cm thick at 1.4 K. The frequency was 9.2 GHz.

faster at smaller inclinations, but we do not find a good $1/\theta$ dependence. Additionally, as illustrated in Fig. 20, the onset of these signals moves to higher field with decreasing θ (whereas the DSCM mode should move to lower field). As mentioned earlier, in our best K sample there was interference between the two modes at the highest field and small angles. This might be indicative of the low-field edge of the DSCM mode, but since our magnetic field was limited to 20 kG we could not verify this possibility by following the signals to still higher fields.

C. Field normal transmission

When the magnetic field is oriented normal to the surface of our alkali samples, there is a rather simple characteristic set of signals. Aside from the conduction electron spin resonance (and spin waves) there appears to be only two major features of the transmission signal. One of these is a very strong, broad resonance centered very close to the cyclotron resonance field. The other is a series of uniformly spaced oscillations in the amplitude, *but not phase*, of the transmitted field. The oscillations extend down to zero field where the observed signal is simply the tail of the anomalous skin effect. We identify the oscillatory signal with the well known GKO, and the strong peak as a consequence of one circularly polarized component undergoing a resonance near the cyclotron condition. We discuss these signals in some detail as they are potentially useful for an independent determination of the Fermi velocity, and because we believe there may be some confusion in the literature concerning the interpretation of such transmission signals at microwave frequencies. Analogous signals for copper interpreted in a somewhat different aspect than the analysis which follows has been reported.[23]

The data points in Figures 21(a) and 21(b) show the transmission signal and modulus, respectively, for a K sample as the field is swept from zero to 8 kG. Figures 22(a) and 22(b) show the extension of these data to 20 kG. The modulus data points represent the result of calculating the square root

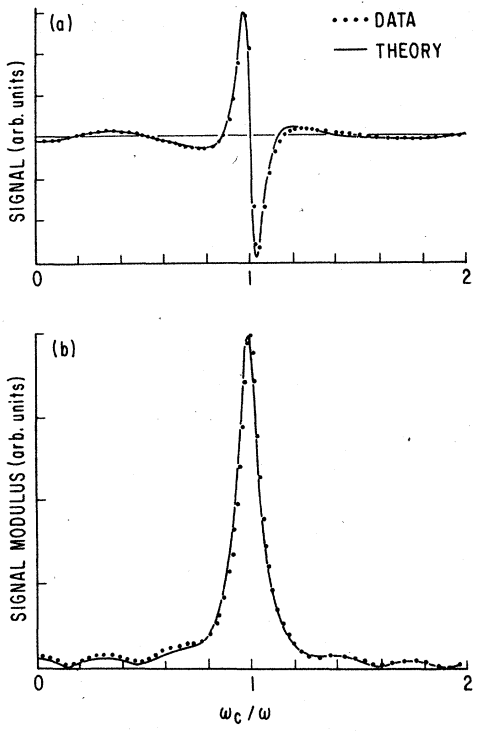

FIG. 21. (a) Transmission signal for a potassium sample when the dc magnetic field is oriented normal to the surface, as a function of the magnitude of the dc field (1–8 kG). The temperature is 1.4 K, the sample thickness 0.012 cm, applied frequency 9.2 GHz. The theoretical curve represents the results of a best fit to the formula of Eq. (3) with the parameters $m^*/m = 1.2$, $\omega\tau = 16.7$, and $\omega\tau_0 = 1.59$. The reference phase was adjusted to yield an antisymmetric big peak signal, as shown, which corresponds to a symmetric CESR signal within a few degrees. (b) Comparison of the signal-modulus data with the computation using Eq. (3) for the same set of parameters as in (a). The curves were normalized at the maximum of the big peak.

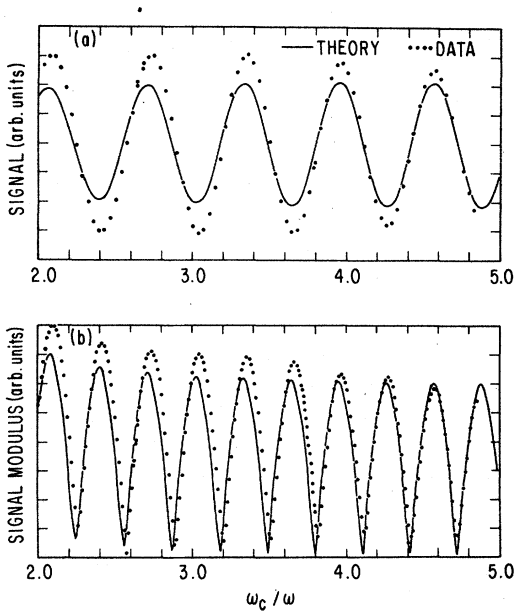

FIG. 22. Continuation onto higher fields (up to 20 kG) for the data and theory as presented in Fig. 21. These values of magnetic field are sufficiently far from that for cyclotron resonance that one sees basically normal Gantmakher-Kaner oscillations.

of the sum of the squares of the signals seen at two phases 90° apart. As we shall discuss in detail later, it is important to observe in Fig. 22(b) that the values of magnetic field for which there is a near zero modulus are the same for which there is a zero crossing in the signal. Changing the reference phase by 90° does *not* interchange peaks and zeros, so that, in brief, the oscillations are not caused by phase changes of h_t relative to the reference field, but rather a true variation of the amplitude of h_t. In our X-band experiments we have also observed similar data as in Figs. 21 and 22 for Na, Rb, and Cs. The big peak has been absent in two Cs samples, although the GKO were present.

The detailed behavior of the signal at the big peak near $\omega_c/\omega=1$ is still not understood, although a large amount of theoretical work has been done.[24] Phillips *et al.* have reported measurements for K at 116 GHz, wherein they observe a strong peak and additional structure near cyclotron resonance. The interpretation of this structure in terms of many-body effects is still uncertain.[25]

Although no satisfactory theoretical formulations exist which accurately reproduce our data, we do find it possible to achieve a very satisfactory fit with a semiempirical formula suggested to us by Wilson.[26] The solid line in Figs. 21 and 22 shows a fit to our data using the formula

$$h_t = Ae^{-(L/v_F\tau)(1-i\omega\tau)} \times\left(\frac{[1-i\omega\tau_0(1-\omega_c/\omega)]^2 e^{-(i\omega_c/\omega)(L/R)}}{[1-i\omega\tau(1-\omega_c/\omega)]^2} + \frac{[1-i\omega\tau_0(1+\omega_c/\omega)]^2 + e^{(i\omega_c/\omega)(L/R)}}{[1-i\omega\tau(1+\omega_c/\omega)]^2}\right). \tag{3}$$

L is the sample thickness, v_F the Fermi velocity, ω the applied microwave frequency, $\omega_c = eH/m^*c$, m^* is the effective mass, R is the cyclotron radius at cyclotron resonance ($=v_F/\omega$), τ is the bulk momentum scattering time, and τ_0 is an assumed different (shorter) scattering time characteristic of a thin layer at each surface. The amplitude factor A includes the phase shift terms due to the surface impedance which are all presumed to be independent of dc field. In reality, Eq. (3) is an asymptotic approximation to a more complete formula that can also contain the Landau A_n parameters, but the full formula fits less well than this approximation, and in light of the theoretical difficulties, it is not worth pursuing these details. The fit in Figs. 21 and 22 were done by adjusting τ to match the width of the big peak at $\omega_c/\omega \cong 1$ and adjusting τ_0 to match the amplitude of the modulus of the observed signal at $\omega_c/\omega = 5$. The fit in Fig. 21(a) could have been made even better with a slight phase adjustment. We note several important features about these data.

(i) The main peak occurs very close to the field for cyclotron resonance. Values of m^*/m deduced from the center of this peak for Na and K are consistently 1 or 2% higher than the cyclotron masses listed in Table I. A similar discrepancy was observed by workers at 116 GHz.[25] If there were a reliable theory to interpret the data, we note that the center of this peak could be found with an accuracy about one order higher than is available for defining cyclotron resonance values of m^*. The value of m^*/m we obtained for Rb is 1.23.

(ii) As can be seen in Figs. 21(b) and 22(b), there are periodic values of the field for which there is zero transmitted power. Equation (3) simplifies considerably if we examine its behavior far away from the big peak. For $\omega_c/\omega \gg 1$, we have

$$E \cong (\tau_0/\tau)^2 e^{-L/v_F\tau} e^{i(\omega L/v_F+\varphi)} \cos(\omega_c L/v_F). \tag{4}$$

Here φ is the adjustable phase introduced by the reference phase shifter. For $\omega_c/\omega \ll 1$, Eq. (3) reduces to a similar expression except that the prefactor $(\tau_0/\tau)^2$ is replaced by a complex function of τ and τ_0. The phase of this prefactor does not alter the field locations for the zeros or maxima of the transmitted field, but it may reverse the sign of the $\omega_c/\omega \ll 1$ peaks as compared to the zero-field extrapolation of Eq. (4). Thus, within the framework of Eq. (3), the only "phase shift" that should occur as one crosses the big peak is either 0 or π, depending on the nature of the relaxation times.

(iii) From an examination of Eq. (4) we shall see that in principle it is possible to determine both v_F and k_F independently from the GKO. Note that all the field dependence in Eq. (4) is in the $\cos(\omega_c L/v_F)$ term, and since $\omega_c \propto 1/m^*$, the spacing in field of the GKO peaks (or zeros) allows a determination of $k_F = m^* v_F$ providing L is known. Alternatively, one may turn this backwards and for the alkalis where k_F is well known, determine L. The practical aspects of determining the thickness this way for the alkalis will be discussed later.

We now come to the question of determining v_F. We illustrate the method by describing a procedure that can be followed. We first note that under conditions where Eq. (4) is applicable it is possible to adjust φ such that the signal is zero for *all values of the dc field.* (i.e., if the spectrometer measures the real part of Eq. (4) then the condition is $\omega L/v_F + \varphi = \pi/2, 3\pi/2, \ldots$.) In our samples with high values of $\omega\tau$ we find we can do this by

simply sweeping the field near 20 kG while changing the phase shifter in the reference arm until a good null phase is found. (In some samples we find there is no phase which gives a true zero of transmission, although there is typically one for minimum transmission. We attribute this to interference with the high-field tail of the big peak. Alternatively, it could be due to a variation in sample thickness.) Returning to the possibility of determining v_F, we note that if one were to change the thickness of the sample and determine the new value of φ which gave a null, one could calculate it from $v_F = \omega \Delta L / \Delta \varphi$.

An alternative procedure would be to change the spectrometer frequency by some amount $\Delta\omega$. One would then also need a phase reference for the spectrometer itself, but this could simply be the CESR signal. We have not done this because the tuning range of our spectrometer is only ~10%, and for a typical sample $\omega L / v_F \sim 10$. Thus there would only be a phase change of one radian, and a high signal-to-noise ratio would be necessary to yield an accurate determination of v_F. The phase can be followed much further by the first method of changing thickness, but we have not tried to do precision measurements at this time because there does not seem to be much need for an independent measurement of v_F in the alkalis. In concluding this topic we wish to emphasize that for the alkalis, when *linear excitation and detection are used*, phase extrapolations to zero field would not be meaningful insofar as v_F determinations are concerned, since the signal is always a local maximum (or minimum) at zero field, independent of the reference phase.[27]

We have attempted to use the field dependence of the GKO to determine the thickness of samples for reasons discussed in the preceding paper.[7] Figure 23 shows a plot of the peak location of the GKO versus the applied magnetic field for a Rb sample. There is a slight deviation from linearity at the lower field where the effect of the big peak is still important. At higher fields (where we also find a phase that gives a zero transmitted field) the line is satisfactorily linear. We have compared the values of the sample thickness deduced from the slopes of lines such as in Fig. 23 with the measured sample thickness for Na, K, and Rb. Initially, using samples of Na and K we thought there was a discrepancy, but this was resolved when it was realized that the packaging between glass plates resulted in the integrated thermal contraction being typically 4% rather than the bulk value of 1.5%. For both Na and K the thicknesses deduced by the GKO do agree with the thicknesses as corrected for the true thermal contraction to within the experimental errors of ±1%.

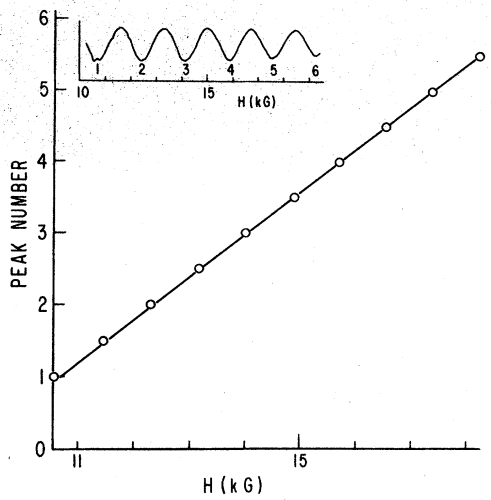

FIG. 23. Peak number of the GKO vs magnetic field for a 0.017-cm rubidium sample at 1.4 K, and a frequency of 9.2 GHz. The inset shows the signal and numbering scheme. Note the slight deviation from linearity at low field, presumably the result of the tail of the resonance at $\omega_c/\omega = 1$.

The situation for Rb appears to be different. The GKO do not yield the same thickness as that determined directly, nor do they give results which even scale consistently with those of either the cyclotron waves or the type-B angular oscillations.[7] This discrepancy may be due to either strain effects, the increasing importance of nonsphericity of the Fermi surface, or possible other mechanisms.

IV. CONCLUSIONS

In addition to the data presented, we have studied all the modes, at least qualitatively, as a function of temperature. If there were interest in the scattering mechanisms, the amplitude could be studied quantitatively as a function of temperature and thickness. Because of the need to determine the thickness of Rb samples, as discussed in Ref. 7, we have checked the dependence of the periodicity of the oscillations observed in the signal for the cyclotron waves, the type-B signals, and the GKO. We have concluded that the periodicity of the first two, as discussed in the text, is a reliable indicator of sample thickness to an accuracy of better than 1% for the three alkalis. This was not true for the GKO.

We have indicated the process whereby we have deduced the A_2 and A_3 coefficients from the cyclotron waves making use of finite $\omega\tau$ dispersion relations and a phenomenological expression for the transmitted microwave field.[9] Surprisingly, our

results (where comparable) are in agreement with those of Walsh *et al.*;[4,14] Since their values were deduced by fitting to an infinite $\omega\tau$ dispersion relation, we had anticipated that there would be appreciable discrepancies, as it is clear that the inclusion of finite $\omega\tau$ effects is essential for the interpretation of transmission measurements. Perhaps the interpretation of reflection data is less affected by finite $\omega\tau$, although the proof of such a conjecture and indeed, a justification of our own data analysis must await a more rigorous solution of the boundary value problem. The extension of these measurements to Cs, or to additional subharmonics for K and Na, is possible, although tedious, and it would require some new theoretical insight to justify the considerable effort involved.

As noted, the signal-to-noise ratio of the GKO at the center of the strong peak is sufficient that the center can be located to at least 0.1%. If this data could be better interpreted in terms of the properties of the system, perhaps a significantly more precise value for m^* could be deduced.

We have reported our observations of a new mode, containing two series, each characterized by a rapid oscillatory dependence of the transmitted field on the angle between the applied dc magnetic field and the sample surface. We tentatively identify one of these series with a model dependent upon the time of flight for electrons along the field lines. The other appears to be more complicated and we suggest that both warrant additional theoretical attention.

Part of our original motivation for studying these modes was to be able to better understand their analogies in metals with more complicated Fermi surfaces. We have observed numerous wiggles in the transmitted signals for every pure metal for which we have searched for CESR. In some cases, such as Ag, Cu, and Al, we can identify parts of the spectrum that bear an obvious resemblance to one or more of the modes discussed here. Other workers have also reported related measurements,[23,28] but given the powerful well-exploited Fermiology tools, such as de Haas–van Alphen, etc., we believe it will take new insights to motivate further detailed measurements.

ACKNOWLEDGMENTS

We wish to thank Professor D. Fredkin and Dr. A. Wilson for many informative discussions, suggestions, and help with the computational expressions. We thank Professor P. Noziéres for an insightful presentation of the origin of the cyclotron waves. We thank C. E. Taylor for supplying the high-purity sodium, and Paul H. Schmidt for his help in purifying the other alkalis. We thank Clancy A. Latham and Donald Eigler for their assistance in technical matters, and John Armstrong for his help in the computer analysis. We acknowledge with appreciation a grant for computer funds from the Research Committee for the San Diego Division of the Academic Senate. This work was supported in part by NSF Grant No. DMR 74-24361.

---

*Present address: Lawrence Livermore Laboratory, P. O. Box 808, Mail Code L-523, Livermore, Ca. 94550.

†Present address: Wayne State University, Dept. of Physics, Detroit, Mich. 48202.

[1]In cgs units, c is the velocity of light, σ is the electrical conductivity, ω is the applied angular frequency, and μ is the permeability.

[2]G. E. H. Reuter and E H. Sondheimer, Proc. R. Soc. Lond. A 195, 336 (1948).

[3]For the ordinary mode see P. M. Platzman, W. M. Walsh, Jr., and E-Ni Foo, Phys. Rev. 172, 689 (1968). For the extraordinary mode see W. M. Walsh, Jr. *et al.*, Proceedings of the Twelfth International Conference on Low Temperature Physics, Kyoto, 1970 (unpublished) and references cited therein.

[4]P. M. Platzman and P. A Wolff, *Waves and Interactions in Solid State Plasmas* (Academic, New York, 1973).

[5]V. F. Gantmakher and E. A. Kaner, Sov. Phys.-JETP 21, 1053 (1965).

[6]D. Pines and P. Nozières, *The Theory of Quantum Liquids* (Benjamin, New York, 1966), Vol. I.

[7]D. Pinkel and S. Schultz, preceding paper, Phys. Rev. B 18, 6639 (1978).

[8]G. L. Dunifer, D. Pinkel, and S. Schultz, Phys. Rev. B 10, 3159 (1974).

[9]See D. Fredkin and A. Wilson, following paper, Phys. Rev. B 18, 6676 (1978).

[10]A comprehensive article on our transmission spectrometer is in preparation. A more detailed block diagram may be found in Ref. 8. A discussion of the mode of operation is presented in *Measurements of Physical Properties*, edited by E. Passaglia, (Wiley, New York, 1972), Vol. IV, Chap. VB, and references cited therein.

[11]There are two criteria. The dc leakage must be negligible compared to the reference, and the modulated leakage must be negligible compared to the signal fields.

[12]The Na used in these experiments was obtained from C. E. Taylor. The K and Rb were refined in our laboratory following the procedure of P. H. Schmidt (private communication). Typical resistivity ratios (300/4.2 K) were: Na 7000–10 000, K 4000–7000; Rb $\cong$2000 (at 300/1.4).

[13]W. M. Walsh, Jr. and P. M. Platzman, Phys. Rev.

[14]See reference b of Table I. (However, see comments in text on their use of the infinite $\omega\tau$ dispersion relations.)
[15]Our numerical values of the fundamental dispersion relation are in agreement with those given in Fig. VIII-14 of Ref. 4, but those for the first subharmonic differ beyond the turning point with the values in their Fig. VIII-18. We have rechecked our calculations and believe that the results presented here are correct.
[16]G. L. Dunifer, P. H. Schmidt, and W. M. Walsh, Jr., Phys. Rev. Lett. 26, 1553 (1971).
[17]J. B. Fransden and R. A. Gordon, Phys. Rev. B 14, 4342 (1976).
[18]R. Freedman and D. Fredkin, Phys. Rev. B 9, 360 (1974).
[19]O. V. Konstantinov and V. G. Skobov, Sov. Phys.-Solid State 13, 2792 (1972).
[20]D. M. Sparlin, Phys. Lett. A 25, 46 (1967).
[21]We note that the breakdown of the agreement between theory and experiment for the spin waves at low $\omega\tau$ is also more pronounced for Rb compared to Na. (See Ref. 7.)
[22]O. V. Konstantinov and V. G. Skobov, Sov. Phys.-JETP 34, 885 (1972).
[23]T. G. Phillips, G. A. Baraff, and P. H. Schmidt, Phys. Rev. B 5, 1283 (1972), and references cited therein. These authors term the peak at cyclotron resonance as "cyclotron phase resonance."
[24]G. A. Baraff, Phys. Rev. B 9, 4008 (1974).
[25]T. G. Phillips, G. A. Baraff, and G. L. Dunifer, Phys. Rev. Lett. 30, 274 (1973).
[26]A. Wilson (private communication).
[27]We note that this behavior is to be contrasted to the data and observations as presented in Ref. 22. In that work with Cu samples, linearly polarized transmit and receive cavities were used, but the authors concluded that the properties of the transmitted signals (at high field) implied that it was predominantly circularly polarized.
[28]J. O. Henningsen, Phys. Rev. Lett. 24, 823 (1970); J. O. Henningsen and D. S. Falk, Phys. Rev. Lett. 26, 1174 (1971); K. Saermark and J. Lebech, Phys. Lett. A 38, 121 (1972). Finite $\omega\tau$ effects in the dispersion relation (but not Landau coefficients) have been included in analysis of cyclotron waves in Ag. J. B. Frandsen, L. E. Hasselberg, J. Lebech, and K. Saermark, Phys. Status Solidi B 67, 501 (1975).